E15-2007-82

M. Majerle[1,2], V. Wagner[1,2], A. Krása[1,2], J. Adam[1,3],
S. R. Hashemi-Nezhad[4], M. I. Krivopustov[3], F. Křížek[1,2],
A. Kugler[1], V. M. Tsoupko-Sitnikov[3], I. V. Zhuk[5]

MONTE CARLO STUDIES OF THE «ENERGY PLUS TRANSMUTATION» SYSTEM

[1]Nuclear Physics Institute of ASCR PRI, 250 68 Řež near Prague,
Czech Republic
[2]FNSPE of CTU, 115 19 Prague, Czech Republic
[3]Joint Institute for Nuclear Research, 141980 Dubna, Russia
[4]School of Physics, A28, University of Sydney, NSW 2006, Australia
[5]Joint Institute of Power and Nuclear Research, Sosny, 220109 Minsk,
Belarus

Майерле М. и др.   E15-2007-82
Исследование методом Монте-Карло системы «Энергия плюс трансмутация»

Установка «Энергия плюс трансмутация» состоит из толстой свинцовой мишени, окруженной урановым бланкетом и помещенной в полиэтиленовый бокс. Свинцовая мишень облучается релятивистскими протонами. Возникающий нейтронный поток исследуется в различных частях установки с помощью активационных детекторов. В работе методом Монте-Карло (MCNPX) исследуются возможные источники систематических экспериментальных погрешностей, возникающих в процессе облучения, в частности, влияние различных частей установки, неопределенности их геометрии и физических свойств. Обсуждаются возможности сравнения экспериментальных данных с результатами расчетов MCNPX.

Работа выполнена в Лаборатории ядерных проблем им. В. П. Джелепова ОИЯИ.

Majerle M. et al.   E15-2007-82
Monte Carlo Studies of the «Energy plus Transmutation» System

«Energy plus Transmutation» setup consists of a thick lead target surrounded with uranium blanket and placed in a polyethylene box. Relativistic protons are directed to the target. Produced neutron flux is studied at different places of the setup using the activation detectors. The possible sources of systematic uncertainties of obtained experimental data are analyzed using MCNPX simulations. Further, the influence of different setup parts and uncertainties in their geometrical and physical definitions on the neutron flux is investigated. The possibility to compare the experimental data with the results of the MCNPX simulation code is discussed.

The investigation has been performed at the Dzhelepov Laboratory of Nuclear Problems, JINR.

INTRODUCTION

Nowadays, there is a great motivation towards improving the precision of the predictions of the Monte Carlo (MC) codes that are used to simulate the production of neutrons in spallation reactions and transportation of high and low energy neutrons in complex nuclear systems. More realistic codes will be invaluable in design of future accelerator driven systems (ADS). The «Energy plus Transmutation» (EPT) international collaboration studies neutron production and transport inside a thick lead target and in the surrounding subcritical uranium blanket when the target is irradiated with high energy protons [1, 2, 3]. The neutron flow of the system was investigated using activation radiochemical detectors. The obtained experimental data are compared with the predictions of the MC codes such as MCNPX [4] or DCM [5].

1. EXPERIMENTAL SETUP

The target–blanket part of the EPT setup [1] is composed of four identical sections. Each section contains a cylindrical lead target (diameter 8.4 cm, length 11.4 cm) and 30 natural uranium rods (diameter 3.6 cm, length 10.4 cm, weight 1.72 kg) distributed in a hexagonal lattice around the lead target. The lead target and uranium rods are enclosed in aluminum claddings of thicknesses 2 and 1 mm, respectively. The target and uranium rods in each section are secured in hexagonal steel container with a wall thickness of 4 mm. The front and back of each section are covered with a hexagonal aluminum plate of thickness 5 mm. The four target blanket sections are mounted along the target axis on a wooden plate (thickness 6.8 cm) covered with 0.4 cm thick steel sheet. There are 0.8 cm gaps between the blanket sections which are used for placement of activation and other detectors. The four target blanket sections mounted on the wooden plate are placed in a wooden container filled with granulated polyethylene, density of which was measured to be 0.8 g cm^{-3}. The inner walls of the polyethylene box are covered with 1 mm thick cadmium layer. The floor wall of the polyethylene box is a textolite plate of thickness 3.8 cm. The polyethylene box and cadmium are used to modify the neutron spectrum as will be discussed in this paper. The geometrical arrangements and dimensions of the EPT setup are shown in Fig. 1.
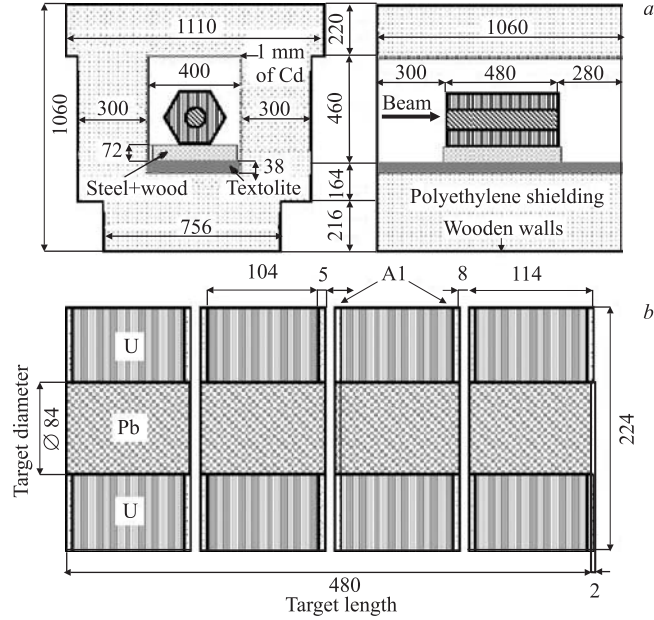
Fig. 1. The layout of the EPT setup: *a*) the front cross section and the side cross section, *b*) the side cross section of the target–blanket only

Several experiments have been carried out using the EPT setup and its target was irradiated with relativistic protons of energies in the range of 0.7 to 2 GeV. In these experiments the neutron flux was measured using activation foils (radiochemical detectors) that were placed between the blanket sections. The radiochemical detectors (aluminum, gold, bismuth, yttrium, and other monoisotopic and nonmonoisotopic stable materials) with dimensions of 2×2 cm^2 and the thickness of ca. 0.1 mm were used. Various nuclear reactions, e. g., (n, γ), (n, xn), (n, α), occur in the radiochemical detectors. The production rates of the reaction products were determined from the intensity of corresponding gamma rays.

For thermal, epithermal, and resonance neutrons, the dominant reaction is the neutron capture (n, γ) process for which cross sections are large (in the range of hundreds to thousands of barns). The others are threshold reactions for which cross sections are in range of mbarns to barns. At the end of the irradiation, the activities of detectors were measured by the means of HPGe detectors and were converted into production rates $B(^{Z}A)$, which give the number of produced nuclei of the isotope A normalized to 1 g of the activation detector and to 1 primary proton [2]. This will be discussed in Sec. 6.

2. SIMULATION PROCEDURE

The MCNPX v2.6.c [6] Monte Carlo code was used to simulate the behavior of neutrons and other secondary particles in the experimental setup. The EPT setup was defined in the code with the characteristics given in Fig. 1 and the specification given in Sec. 1. Figure 2 illustrates the EPT setup as seen by the MCNPX code. Figure 2, a shows the MCNPX plot of the XY (a plane normal to the target axis, Z) cross section of the EPT setup, and in Fig. 2, b the YZ cross section of the EPT is shown. In Fig. 2, b the control detectors with their corresponding reference numbers are added to the MCNPX plot.
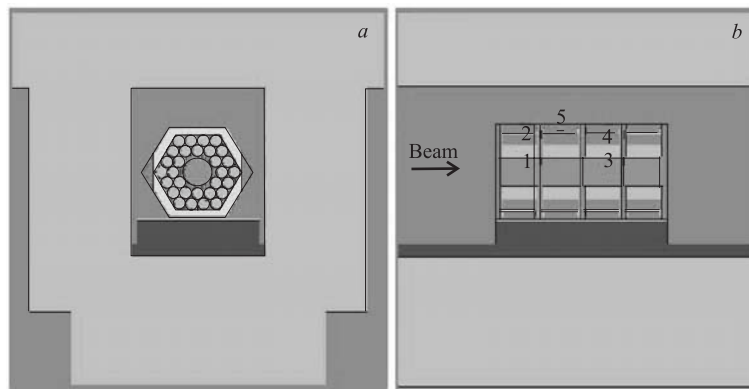
Fig. 2. a) The front cross section of the target placed in the polyethylene box (MCNPX plot). b) The side cross section of the target placed in the polyethylene box (MCNPX plot) with enumerated control detectors

In order to obtain $B(^Z A)$ production rates at different places of the setup, the simulated spectra of neutrons, protons and pions were convoluted with the cross section for the specific reaction. Because the cross sections for (n, xn), (n, f), (n, α) reactions, and reactions with protons and pions are either not included in MCNPX cross section libraries or are limited in the energy range, the missing cross sections were previously simulated (calculated with MCNPX and CEM03 intranuclear cascade model, extracted with FT8 RES card). Afterwards, the simulated neutron, proton, and pion spectra (in MCNPX they are obtained with the F4 tally card, the energy bins are set with E4 card) at the places of the control detectors were convoluted with these cross sections. In the case of the (n,γ) reactions the cross sections from the MCNPX libraries were used.

In order to investigate the effect of different parts of the experimental setup on the obtained results, simulations with changed geometrical and physical properties of the setup were performed. The influence of the Intra-Nuclear Cascade (INC) model and the cross-section libraries was estimated by series of calculations with different libraries and INC models. MCNPX was also used to calculate the

3

criticality of the experimental setup, as well as the number of produced neutrons per one incident proton. These two parameters are crucial when comparing the EPT setup with similar ones.

2.1. Control Detectors. Five thin gold foils were used as control detectors in simulations. Foils 1 and 2 were placed in the first gap between the target blanket sections, at the radial distances of 3 and 11 cm from the target axis. The foils 3 and 4 were at the same radial positions as the foils 1 and 2, but in the third gap. The foil 5 was in the horizontal position on the top of the second blanket section. The positions of the control detectors are shown in Fig. 2, *b*.

In the control detectors (foils) two reactions with neutrons in gold were simulated: ^{197}Au(n, γ)^{198}Au and ^{197}Au(n, $2n$)^{196}Au. The reaction ^{197}Au(n, γ)^{198}Au is sensitive to the low-energy neutrons ($E_n < 0.1$ MeV) while the ^{197}Au(n, $2n$)^{196}Au reaction has a threshold energy of 8 MeV and therefore shows the behavior of the high-energy neutrons ($E_n > 8$ MeV) in the EPT setup. The variation of the production rates of these two isotopes by altering the parameters of the experimental setup was investigated. The calculations were performed when the incident proton energy was 1.5 GeV.

3. THE INFLUENCE OF THE SETUP PARTS AND EXPERIMENTAL CONDITIONS ON THE NEUTRON SPECTRUM

3.1. The Influence of the Polyethylene Box and Cadmium Layer. The polyethylene box around the target–blanket moderates part of the neutrons and
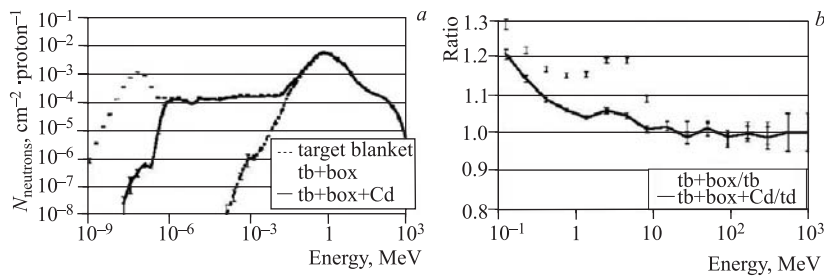
Fig. 3. *a*) The simulated neutron spectra on top of the second section of the target–blanket are shown for three cases: for the target–blanket without the polyethylene box, for the target–blanket with the box but no cadmium (tb+box), and for the target–blanket with both, the box and the cadmium (tb+box+Cd). Small thermal peak in the case of tb+box+Cd is caused by the moderation effect of the wood. *b*) The ratios of the spectra from the left figure from the energy 0.1 MeV. From these ratios it can be concluded that the polyethylene box affects significantly only neutrons with energies lower than 10 MeV. The increase of the ratios in 1–10 MeV range is caused by the fission of ^{235}U with moderated neutrons

reflects them back inside the box. The 1 mm thick cadmium sheet that covers the

4

inner walls of the polyethylene box absorbs most of the reflected slow neutrons. A set of simulations (without box, with box but no cadmium, and with both — box and cadmium) showed that only reflected neutrons with energies less than 10^{-6} MeV are stopped by the cadmium layer (Fig. 3, a). The box and cadmium do not affect by more than a few percent high energy ($E_n > 10$ MeV) part of the neutron spectrum (Fig. 3, b). From Fig. 3 is evident that the low-energy part of the neutron spectrum in the blanket area has been produced by the combined effects of the polyethylene and cadmium around the target–blanket system. The spectra shown in Fig. 3 were calculated on top of the second section of the target–blanket.

3.2. The Influence of Other Setup Parts (Metal Parts, Wood). Experimental data have shown that at the bottom part of the target–blanket system there are more low-energy neutrons than at its upper part [8]. To verify if this is due to the wooden and textolite plates under the target–blanket system, the following three simulations were performed:

1) both wooden plate and polyethylene box were present,

2) only wooden plate was present,

3) only polyethylene box was present.

Fourteen ^{197}Au detectors were placed in the first gap along the vertical axis Y in the interval from –14 to 14 cm and ^{196}Au, ^{198}Au production rate in each detector was determined. The wooden and textolite plates were approximated with the wood from the MCNPX materials library [9] and atomic fractions of 51, 23, and 26% were used for H, C and O, respectively. The same density of 0.5 kg/l was used for the wood and textolite. The calculation results are shown in Fig. 4. In the case of the high-energy neutrons, no asymmetry beyond
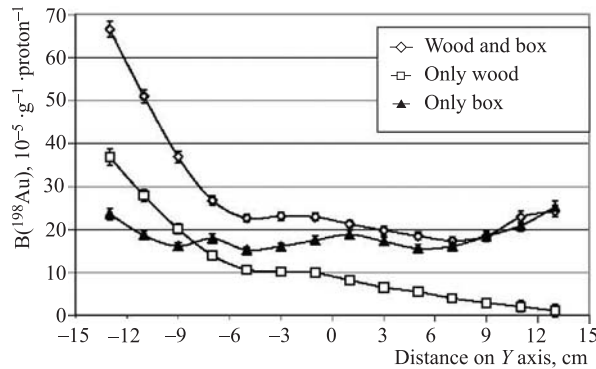
Fig. 4. The ^{197}Au$(n,\gamma)^{198}$Au production rates in detectors placed along the vertical axis Y in the first gap. The MCNPX calculations were performed for three different material compositions of the EPT setup as shown in the figure inset

the 5% was observed between the ^{196}Au production rates in the Au-detectors in $+Y$ direction as compared to their corresponding detectors in the $-Y$ direction. However, in the case of the low-energy neutrons the ^{198}Au production rate is dramatically affected by the presence of the wooden and textolite plates. The polyethylene box alone (in absence of the wooden and textolite plates) produces almost homogeneous, low-energy neutron field in the first gap. This is expected due to the geometrical and material symmetry of the EPT setup in absence of wooden and textolite plates.

The metallic materials (steel and aluminum) used in the target–blanket sections (as described in Sec. 1) do not have significant effect on the neutron spectrum within the blanket. In general, the effects of these parts on the reaction rates in the control detectors do not exceed the statistical uncertainties of the calculations which were about 3%.

3.3. The Influence of Detector Self-shielding. The detectors that were used in the experiments had small dimensions and thus, no significant neutron flux self-shielding is expected. However, some extreme cases where the detectors could influence the experimental results were studied.

With the detector type and dimensions used in the experiments, in principle the detectors in one gap should have negligible influence on detectors in other gaps or on those detectors outside of the target–blanket assembly. This was proved by placing gold foils with thicknesses of 2 and 4 mm in the first gap (extended over the whole gap) and calculating the reaction rates in the detectors in the third gap (i. e., foils 3 and 4 in Fig. 2, b). No significant effects on the reaction rates outside of the 3% statistical uncertainties were observed.

A gold strap of 2 cm wide and 0.1 mm thick, stretching over the whole gap was placed in front of the detectors in the first gap. Subsequent simulations showed that the rate of the ^{197}Au$(n, \gamma)^{198}$Au reaction in the detectors behind gold strap was reduced by up to 15%, while the rate of the ^{197}Au$(n, 2n)^{196}$Au reaction did not change within the statistical uncertainties (3%). The strap should not have any significant effect on the high energy part of the neutron spectrum, as neutrons at that energy have small cross sections for the reactions with the gold. Only the influence of the low-energy neutrons with large cross-section resonances with the gold is expected.

Calculations also showed that when gold foils were covered on both sides with bismuth foils of 1 mm thickness the production rates of the threshold reactions do not change beyond the calculation uncertainties. On the other hand, absorption in gold has significant effect on reactions with low-energy neutrons, i. e., ^{198}Au production rates in 50 μm thick gold foils are 50% lower due to self-absorption. Self-absorpion for threshold reactions is negligible. This suggests that the threshold detectors can be mounted one after another within the gaps.

In the earlier experiments with the EPT setup, the activation detectors were mounted on a thick plastic plate, and then placed in the gaps between the blanket

6
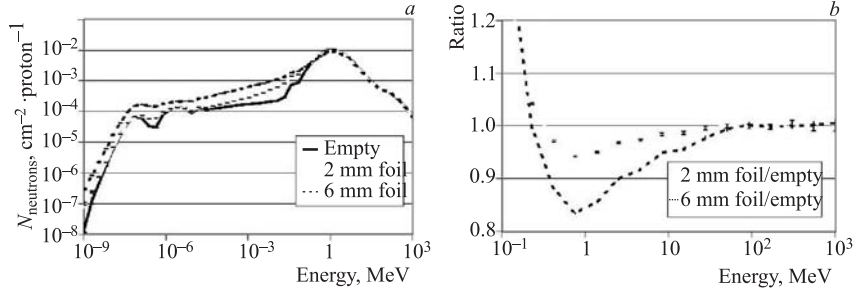
Fig. 5. *a*) The neutron spectra inside the first gap when 2 or 6 mm thick polyethylene foil is inserted in it and with the empty gap (MCNPX simulation). *b*) The ratio of the high energy regions of the spectra from the left figure. It is seen that the polyethylene influences significantly only on neutrons with energies lower than 10 MeV

sections. Such an arrangement may affect the low-energy section of the neutron spectrum in the gaps. MCNPX calculations of the neutron spectrum in the gap in which a polyethylene plate of 2 or 6 mm thickness is inserted showed that such a plate has no effect on the high-energy neutrons ($E_n > 10$ MeV), but changes the low-energy part of the spectrum (see Fig. 5).

Another source of the systematic experimental error is the displacement of the detectors. By simulations it was estimated that a displacement of detectors for 0.5 cm in any direction results in reaction rates that are ca. 20% different from the reaction rates with not displaced detectors.

3.4. The Influence of Beam Parameters on the Reaction Rates. The beam parameters in our experiments were experimentally determined. The beam is usually approximated with the Gaussian distributions in X and Y directions, and its displacement is known with an accuracy of 3 mm. In reality, the beam is Gaussian with the extending tails. To estimate the systematic uncertainty resulting from Gaussian beam approximation and the beam displacement, a set of MCNPX simulations was performed and the reaction rates in the control detectors were computed.

To avoid the influence of the neutrons reflected from the polyethylene box around the target–blanket system, calculations were performed without the polyethylene box. Three calculations were made with two circular and homogeneous beams of 3 mm and 3 cm diameters and with a beam of Gaussian profile for which the FWHM in both X and Y directions were 3 cm. In all three cases the beam directions were parallel to the target axis and the beams and target centers coincided. The induced reaction rates in the control detectors for these three proton beam profiles were the same within the statistical uncertainties of the calculations (i. e., 5%). This suggests that in our experimental setup the beam profile is not of a great importance as long as it is symmetric. The tails of the

beam are for ca. three orders less intensive than the beam central part and have negligible influence on the control detectors.

In a series of calculations without the polyethylene box, the center of the Gaussian proton beam as described above, was displaced by 3, 5, 8, and 10 mm from the target axis and along the positive direction of the Y axis. The reaction rates in the control detectors showed a strong dependency on the beam displacement. The beam displacement of 5 mm changes ^{197}Au$(n, 2n)^{196}$Au and ^{197}Au$(n, \gamma)^{198}$Au reaction rates by up to 20 and 30%, respectively.

With the presence of the polyethylene box (i.e., the case of the actual experiments) and as a result the contribution of the reflected low-energy neutrons, the difference in the ^{197}Au$(n, \gamma)^{198}$Au reactions rates for the cases of centered and displaced beam decreases to about 10% as compared with about 30% when the box was absent. The polyethylene box has no effect on high energy induced reaction rates (i.e., ^{197}Au$(n, 2n)^{196}$Au). A beam centre displacement of 3 mm results in a systematic error of up to 15%. Figure 6, a shows the difference between the reaction rates for centered and displaced proton beams (see the figure caption for details).
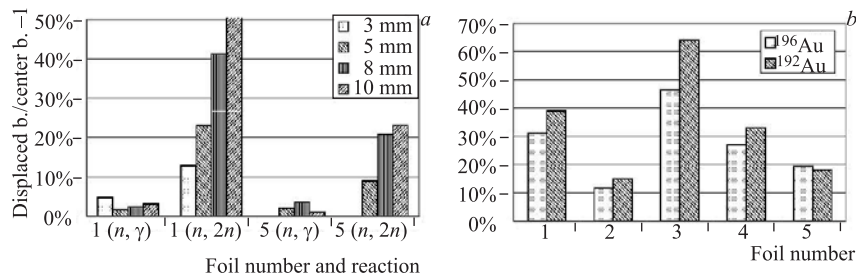
Fig. 6. a) The difference between the reaction rates for centered and displaced proton beams. The proton beam was displaced along the positive Y axis with the amount given in the figure inset, and calculations were performed when the polyethylene box was present. Foils were placed as seen in Fig. 2, b. The abbreviations $(n, 2n)$ and (n, γ) refer to ^{197}Au$(n, 2n)^{196}$Au and ^{197}Au$(n, \gamma)^{198}$Au reactions, respectively. b) The difference between the reaction rates for the beam parallel to the target axis and for the beam entering at $3°$. The abbreviations ^{196}Au and ^{192}Au refer to ^{197}Au$(n, 2n)^{196}$Au and ^{197}Au$(n, 6n)^{192}$Au reactions, respectively

Another calculation was performed with the beam which was not parallel to the target axis. The beam and the target centers coincided, but the direction of the beam was deflected from the target axis for $3°$ upwards, exiting the target from 2.5 cm to its center. Simulation showed that the deflection of the beam causes the increase of the reaction rates for up to 40 and 60% in ^{197}Au$(n, 2n)^{196}$Au and ^{197}Au$(n, 6n)^{192}$Au reactions, respectively (Fig. 6, b).

8

4. ISOTOPE PRODUCTION IN REACTIONS WITH PROTONS, PIONS, AND PHOTONS

Radioactive isotopes in the detectors can also be produced by other particles, mainly by protons, pions, and photons. To estimate the contributions of these particles to the reaction rates in activation detectors, the corresponding reaction cross sections were evaluated using the MCNPX. The neutron, proton, pion and photon spectra in the control detectors were calculated and then were convoluted with the evaluated cross sections. It was found that up to 20% of reaction products could be produced by proton induced reactions suggesting that the influence of protons cannot be neglected. The isotope production by pions and photons is at least one order of magnitude lower than isotope production with neutrons, and their influence can be neglected. Most of these contributions are proton induced reactions from primary beam. The contribution of radioisotopes produced by protons decreases very quickly with increasing radial distance and is strongly dependent on the proton beam profile and position of the beam center on the target.

5. PARAMETERS OF THE SIMULATIONS: EFFECTS OF DIFFERENT PHYSICS MODELS AND CROSS-SECTION LIBRARIES

In MCNPX, spallation reaction is simulated in three steps: intra-nuclear cascade (INC), pre-equilibrium stage, and evaporation stage [10]. The setup was simulated with different combinations of INC (cem03, Bertini, Isabel, incl4) and evaporation models (Dresner, ABLA), in order to check if these combinations of built-in models predict similar reaction rates. The model responsible for pre-equilibrium stage cannot be manipulated in MCNPX.

In the case of ^{197}Au$(n, 2n)^{196}$Au reaction, different INC models predict reaction rates similar within 10% when using the same evaporation model. These reaction rates differ for 40% from the reaction rates calculated with another evaporation model. The situation for the ^{197}Au$(n, 6n)^{192}$Au reaction with higher threshold ($E_{\mathrm{thr}} = 39$ MeV) is inverse, only the use of different INC model changes the results significantly, while the results are not changed if another evaporation model is used.

New cross-section libraries NRG-2003 [11] are available up to 200 MeV in the MCNPX code package recently, apart from the standard LA150 libraries [12], which are available up to 150 MeV. Simulations confirmed that the reaction rates calculated using the cross sections from NRG-2003 libraries are the same as the reaction rates calculated using the standard LA150 libraries within few percents.

6. COMPARISON OF EXPERIMENTAL DATA AND CALCULATION RESULTS

Figure 7, a shows the spatial distribution of some threshold reaction rates (the B values) in the gold at the incident proton energy of 1.5 GeV. The gold detectors were placed within the first gap at radial distances of 3, 6, 8.5 and 13.5 cm. The threshold energy for (n, xn) reactions, ($x = 2$ to 7) are in the range from 8 to 40 MeV. The B values for all reactions rapidly decrease with increasing distance from the target axis.
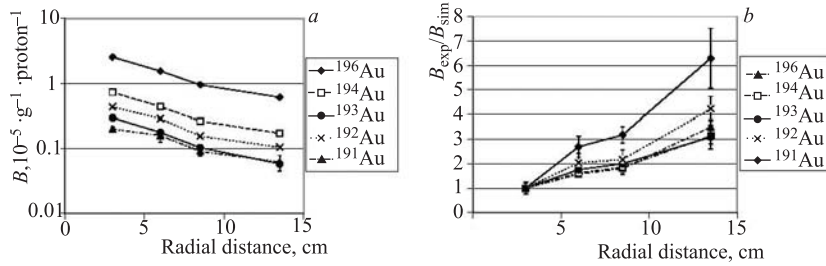
Fig. 7. a) The radial distributions of the experimental reaction rates (B values) in gold detectors placed in the first gap. The lines are drawn to guide the eyes. The statistical uncertainties of the points are not visible on this scale. b) The ratios between the experimental values (from Fig. 7, a) and simulated B values. The ratios are normalized to that of the detector at radial distance of 3 cm

The reaction rates were calculated using the MCNPX with the CEM03 model. The ratio between the experimental and calculated results ($\kappa = B_{\mathrm{exp}}/B_{\mathrm{sim}}$) increases with increasing of radial distance and it is more pronounced for reactions with higher threshold energy (Fig. 7, b). In Fig. 7, b all κ values for a given reaction are normalized to that of the detector at 3 cm radial distance. For gold detectors placed at radial distance of 13.5 cm the experimental results are higher than calculated ones by a factor of 3–7. The increase of κ is observed on smaller scale also in longitudinal direction for the detectors placed 3 cm from the target central axis. Reasons for such large discrepancies are under investigation.

7. SIMULATION OF THE GLOBAL CHARACTERISTICS OF OUR SETUP

Two important parameters of the EPT setup were determined with simulations: the criticality (k_{eff}) and the number of produced neutrons per one incident proton. Using KCODE, the criticality of the EPT setup was calculated to be $k_{\mathrm{eff}} = 0.20247$. At the energy $E_p = 1.5$ GeV the overall neutron production per incident proton m is 50, which is the sum of the number of neutrons escaped
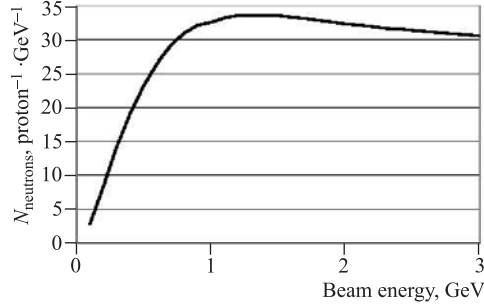
Fig. 8. Dependence of the number of produced neutrons in the whole setup on the energy of the protons, normalized to one proton and to one GeV of proton energy (MCNPX simulation)

from the setup and the number of neutrons captured in the setup. But in Fig. 8 the ratio of m/E_p is shown as a function of incident proton energy (E_p). As can be seen the optimal energy for the neutron production is around 1 GeV.

CONCLUSION

The «Energy plus Transmutation» setup is used for the studies of neutron production and transport, transmutation of radiative materials and other aspects of accelerator driven systems. The neutron flow of the system is studied with activation radiochemical detectors. In this paper, it is shown that the experimental data for higher energies ($E > 10$ MeV) from this type of detectors are not influenced (within the accuracy of 5%) by the polyethylene box, the material of different holders, other construction details, or by the detectors. The systematic uncertainty mostly depends on the beam and detector displacement — the inaccuracies of 3 mm in beam or detector position bring each ca. 15% systematic uncertainty in the production rates. The dominant sources of epithermal, resonance, and thermal neutrons are moderation and scattering of the neutrons in the polyethylene box. Therefore, the flux of low-energy ($E < 0.1$ MeV) neutrons is almost homogeneous at the place of the target–blanket assembly. The MCNPX calculations showed that the experiments with the EPT setup provide valuable data with experimental uncertainties within the range of 30% for high energy part of the neutron spectrum ($E > 10$ MeV), studied by threshold detectors.

The differences between the experimental values and the values calculated with the MCNPX are within the limits of the experimental uncertainties for the experiments with 0.7 and 1 GeV proton beams, but the experimental values for the experiments with 1.5 and 2 GeV proton beams were few times higher than the

11

simulated values. These differences are not within the limits of the experimental uncertainties and are being investigated.

REFERENCES

1. *Krivopustov M. I. et al. //* Kerntechnik. 2003. V. 68. P. 48.

2. *Krivopustov M. I. et al.* JINR Preprint E1-2004-79. Dubna, 2004.

3. *Křížek F. et al. //* Czech. J. Phys. 2006. V. 56. P. 243.

4. Group X-6, MCNPX 2.3.0 -Monte Carlo N-Particle Transport Code System for Multiparticle and High Energy Applications. Los Alamos; New Mexico: LANL 2002.

5. *Barashenkov V. S. //* Comp. Phys. Comm. 2000. V. 126. P. 28.

6. *Hendricks J. S. et al.* MCNPX, version 2.6.c, LA-UR-06-7991.

7. *Mashnik S. G. et al. //* J. Phys. Conf. Ser. 2006. V. 41. P. 340–351.

8. *Zhuk I.* Private communication.

9. *Griffin M. A.* Private communication.

10. *Cugnon J.* Cascade Models and Particle Production: A Comparison. Particle Production in Highly Excited Matter. ISBN 0-306-44413-5 // NATO Science Series. B. 1993. V. 303. P. 271–293.

11. *Koning A. J. et al. //* Proc. of the Intern. Conf. on Nuclear Data for Science and Technology. Santa Fe, USA, Sept. 26–Oct. 1, 2004.

12. *Chadwick M. B. et al. //* Nucl. Sci. Eng. 1999. V. 131, No. 3. P. 293.